ZEBRAFISH
Volume 16, Number 3, 2019

DOI: 10.1089/zeb.2017.1520

Three-Dimensional Printing of Vitrification Loop Prototypes for Aquatic Species

Nolan J. Tiersch,[1] William M. Childress,[2] and Terrence R. Tiersch[2]

Abstract

Vitrification is a method of cryopreservation that freezes samples rapidly, while forming an amorphous solid (''glass''), typically in small (μL) volumes. The goal of this project was to create, by three-dimensional (3D) printing, open vitrification devices based on an elliptical loop that could be efficiently used and stored. Vitrification efforts can benefit from the application of 3D printing, and to begin integration of this technology, we addressed four main variables: thermoplastic filament type, loop length, loop height, and method of loading. Our objectives were to: (1) design vitrification loops with varied dimensions; (2) print prototype loops for testing; (3) evaluate loading methods for the devices; and (4) classify vitrification responses to multiple device configurations. The various configurations were designed digitally using 3D CAD (Computer Aided Design) software, and prototype devices were produced with MakerBot® 3D printers. The thermoplastic filaments used to produce devices were acrylonitrile butadiene styrene (ABS) and polylactic acid (PLA). Vitrification devices were characterized by the film volumes formed with different methods of loading (pipetting or submersion). Frozen films were classified to determine vitrification quality: zero (opaque, or abundant crystalline ice formation); one (translucent, or partial vitrification), or two (transparent, or substantial vitrification, glass). A published vitrification solution was used to conduct experiments. Loading by pipetting formed frozen films more reliably than by submersion, but submersion yielded fewer filling problems and was more rapid. The loop designs that yielded the highest levels of vitrification enabled rapid transfer of heat, and most often were characterized as being longer and consisting of fewer layers (height). 3D printing can assist standardization of vitrification methods and research, yet can also provide the ability to quickly design and fabricate custom devices when needed.

Keywords: 3D printing, vitrification, aquatic species

Introduction

Innovation followed by customization and standardization is necessary for aquatic species to advance in internationally practiced fields such as cryopreservation. Conventional cryopreservation relies on a relatively slow formation of crystalline ice (''equilibrium freezing''), while vitrification rapidly releases heat to form an amorphous solid (glass).[1] Vitrification typically exposes samples to liquid nitrogen, providing a rapid and efficient method of cryopreservation. Sample integrity is preserved against cryogenic temperatures by the addition of concentrated vitrification solutions, in balance with their potential toxicity to cells or tissues.[2] Desirable chemicals for use in vitrification solutions possess properties promoting glass formation, and because of its simplicity, vitrification can be performed in remote locations with minimal instrumentation requirements.[1]

The ability to work in diverse settings, including fieldwork, is crucial to efforts for conservation of endangered species, and vitrification offers an effective way to freeze and store samples for laboratory use with aquatic biomedical models. Despite this, vitrification is underutilized in aquatic species due to the dearth of suitable devices. Available devices often lack essential features such as appropriate sizing, ease of handling, and affordability for new applications such as freezing of fish gametes or embryos.[3] The lack of suitable vitrification devices has constrained research to being performed with devices made for other purposes, such as inoculation loops used in microbiology[4] or plastic strips used for human embryos.[5] Three-dimensional (3D) printing may be a

[1]St. Michael the Archangel High School, Baton Rouge, Louisiana.
[2]Aquatic Germplasm and Genetic Resources Center, School of Renewable Natural Resources, Louisiana State University Agricultural Center, Baton Rouge, Louisiana.

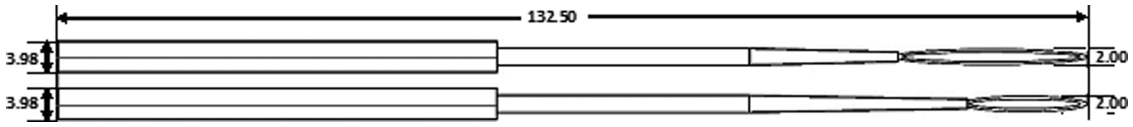

FIG. 1. Examples of schematic diagrams used to design 3D printed vitrification loop prototypes. Widths of all loops were the same, but the length of the loops (at the end of the handles) varied between 23.5 mm (Long; *top*) and 15 mm (Short; *bottom*). 3D, three dimensional.

practical method to address the lack of viable vitrification devices, by fabrication of devices specifically designed for vitrification in aquatic species.

3D printing technology is just beginning to be applied to cryopreservation,[6] and as such the experiments in this study addressed essential nonbiological aspects of materials, design, fabrication, and testing of prototype configurations (loops), and did not involve gametes. A published vitrification solution was used to examine the feasibility of using 3D printed loops to produce vitrification. Acrylonitrile butadiene styrene (ABS) and polylactic acid (PLA)[7] are the most common thermoplastic filament materials, and most 3D printers currently available are compatible with them. They can withstand the extreme temperature changes associated with liquid nitrogen exposure, and thus were the logical choices for this work.

For extrusion, the thermoplastic filament is guided into the 3D printer head and heated to a molten state. The mobile printer head ejects the molten filament onto a build platform at a controlled rate. The filament is stacked in thin layers and hardens to produce designs exported from 3D CAD (Computer Aided Design) software. Engineering of devices for specified applications requires tradeoffs, a system of balancing unwanted with desired qualities. We chose to evaluate 3D printed devices that were constrained in size to fit within the dimensions of a standard cryopreservation container, the 0.5-mL French straw (IMV Technologies, Paris, France). Thus, this work was focused on design, fabrication, and feasibility testing of 3D printed loops for the first time for vitrification.

Given that the goal of this project was to create custom 3D printed open vitrification devices that could be efficiently used and stored, our objectives were to (1) design prototype vitrification loops with varied dimensions; (2) print prototype loops for testing; (3) evaluate loading method for the devices; and (4) classify vitrification responses to multiple device configurations. Relatively long and thin loops proved to be most effective to produce glass when using vitrification solution in volumes of 1 to 19 μL. The prototype loops and methods used in this study offer a path to standardization for cryopreservation of aquatic species by utilizing the increasingly widespread availability and reproducibility of 3D printing.

Materials and Methods

Design of prototype vitrification loops with varied dimensions

Our design criteria were to create (1) devices with dimensions that fit within those of a 0.5-mL French straw; (2) varied loop dimensions to hold a range of film volumes; and (3) triangular handles to facilitate processing and storage. Although these prototype devices were of the same total lengths, handle lengths were varied to allow for differences in loop length (Fig. 1).

Initially, a wide variety of early prototype test devices were digitally designed with various loop dimensions by use of commercially available 3D CAD software (Autodesk Inventor® professional 2016—student edition, San Rafael, CA). The basic design was an elliptical loop at the end of a handle. Eventually, a series based on a total of 18 different loop configurations was selected for further study, with a total length of each device (handle and loop) set at 132.5 mm. The loops were designed as ellipses with a width of 2 mm (outer dimension). Loop configurations comprised three nominal lengths (short, 15 mm; intermediate, 19 mm; and long, 23.5 mm) (Fig. 2), and six nominal heights (0.2, 0.4, 0.6, 0.8, 1, and 1.2 mm) produced by printing of 1–6 layers (0.15–0.2 mm/layer).

Printing of prototype loops for testing

The types of thermoplastic filament materials used to produce the prototype loops were ABS and PLA (Makerbot Industries, Brooklyn, NY) and are available at a cost of about $20–48 per kg. The spools of filament (1.75 mm diameter) were stored in a 63-L plastic bin with a latched lid (Hefty, 7105HFT-10-111-44, Macedon, NY) with desiccant (DampRid, FG01K, Memphis, TN) to minimize humidity. Two MakerBot® 3D printers

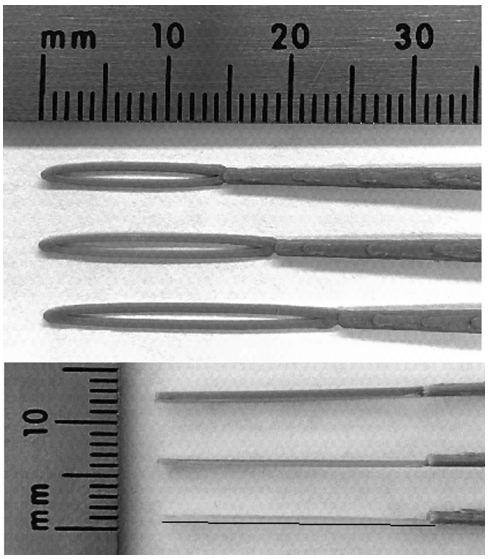

FIG. 2. The loop configurations consisted of one to six layers (nominal 0.2 mm/layer) and three loop lengths (short—15 mm, intermediate—19 mm, and long—23.5 mm). *Top view*: short, intermediate, and long loops (ABS). *Side view*: long loops printed with 6, 3, or 1 layer. A reference line was used to assist visualization of the side view of the single-layer loop (*bottom*). ABS, acrylonitrile butadiene styrene.

(Replicator 2—PLA filament printer, and Replicator 2X—ABS filament printer, New York, NY) were used to produce a total of 72 prototype loops, by printing two replicates of each configuration (3 lengths × 6 heights × 2 thermoplastics). The print time for each device was roughly 3 min, as loop configurations slightly affected print times (1–2 s/layer). The rate of failure to print two replicates of each device was calculated by dividing the number of failed prints by the total number of prints [No. of failed prints(x)/total number of prints]. To further regulate humidity levels, a dehumidifier (Haier, DE45EM-L, Qingdao, China) was constantly operated inside the room where the 3D printers were located. The room used for printing was held at a humidity level between 45% and 55% and the temperature ranged between 22°C and 26°C.

A slicer software (MakerBot Desktop 3.10) was used to import STL (STereoLithography) files of prototype loop designs and control the settings of the printers. Printer settings were adjusted to extrude at 150 mm per sec and retract at 25 mm per sec, with a layer height of 0.20- and 0.48-mm layer width. Both MakerBot printers used an enclosed-fan printing head with a 0.4-mm brass nozzle at 230°C. The printers laid filament onto glass build plates covered with 72-mm wide (nominal 3-inch) blue painter's tape (Scotch™, 2090-72A, St. Paul, MN) with a 25% infill in a hexagonal pattern. The Replicator 2X (ABS) used a heated build plate set at 110°C, while the Replicator 2 used an unheated build plate. The mass of individual devices across the configurations printed for testing averaged ~0.55 g for PLA and ~0.45 g for ABS, yielding a material cost of ~$0.0125 each and cost of around $0.0008 per μL of sample (based on use of a 15-μl device).

Evaluation of loading methods

Characteristics of the two loading methods (pipetting and submerging) were evaluated with two solutions (deionized water and vitrification solution) and multiple loop configurations. The configurations included filament type (ABS or PLA), loop length (short, intermediate, and long), nominal layer height (0.2, 0.6, and 1.2 mm), and loading method. Minimum and maximum capacities (volumes) of loops were calculated with deionized water and vitrification solution. Minimum volumes by pipetting were recorded as the minimal required volume to form a stable film within a loop. Maximum volumes by pipetting were identified as when liquid film levels aligned flush with the top and bottom layers of the loops. Volumes of loaded films were measured by the difference in mass before and after prototype loops were submerged into deionized water or vitrification solution. An analytical balance (Mettler, AE 166, Columbus, OH) was used to determine the mass (mg) of each film. The recorded masses were converted into volumes in μL using the relationship between mass and volume of deionized water (1:1 at 4°C, corrected for testing at 24°C). Known volumes of vitrification solution were compared to equivalent volumes of deionized water to yield a relationship for conversion (volumes to masses) between deionized water and vitrification solution.

Classification of vitrification quality

The vitrification solution chosen was published previously[4] for vitrification of fish sperm (20% 1,2-propanediol +20% 2-methoxyethanol +20% HBSS300 + 40% methanol). Hanks' balanced salt solution at an osmolality of 300 mOsmol/kg was used as a diluent (HBSS300: 0.137 M NaCl, 5.4 mM KCl, 1.3 mM $CaCl_2$, 1.0 mM $MgSO_4$, 0.25 mM Na_2HPO_4, 0.44 mM KH_2PO_4, 4.2 mM $NaHCO_3$, and 5.55 mM glucose, pH 7.2). All solutions were stored at 4°C between testing, and were thoroughly mixed before each use.

Classifications of vitrification quality were assigned to frozen films formed with vitrification solution by each loading method. Only the maximum and minimum volumes required to form films were pipetted into the sampled range of vitrification devices; however, all loop configurations were tested by submersion. A limited range of configurations was loaded by pipetting because of the extended time it took to employ this method. Thus, we formed two film classifications for the minimum and maximum volumes loaded by pipetting, to match the four assessments loaded by submersion.

Two people (assessor and recorder) were used to assign classifications and record thaw times. The assessor removed a vitrification loop from liquid nitrogen and said ''start,'' which informed the recorder to start a timer. The assessor then voiced the classification and the recorder monitored the time to ensure all assessments were made within 2.5 s. The assessor observed the film until thawing and voiced ''stop'' to inform the recorder to stop the timer. The recorder documented the loop configuration, vitrification classification, time to assess, and thaw time. The maximum time to assess a sample was set at 2.5 s to ensure accurate classifications before thawing. This required a trained assessor[8] with experience in handling the devices and classification of the test solutions. A walk-in refrigerated room held at 4°C–7°C with 65%–70% relative humidity was used to assess the samples.

Vitrification quality was measured by the degree of film clarity determined by viewing parallel horizontal lines through frozen films (Fig. 3). A 3D printed pedestal was used for a visual method of classifying vitrification quality.[8] Loaded loops containing films were plunged vertically into liquid nitrogen and held stationary until all bubbling stopped. After the films were frozen, the entire device was stored in liquid nitrogen for at least 1 h. Frozen films were assigned a classification number: zero (opaque, or abundant crystalline ice formation); one (translucent, or partial vitrification), or two (transparent, or substantial vitrification, glass). ''Film fractures'' were recorded when visible cracks disabled the ability to properly assign a numerical classification; however, partial vitrification could be present between the cracks. ''Film failures'' were recorded when films were disrupted during the freezing process, and sometimes, residual sample was observed at the ends of the loops (Fig. 3). An additional relevant concept was identified as a ''filling failure,'' which occurred when initially loading a loop, before freezing, but this was recorded as a component of the time required to fill the loops and was not isolated as a data category.

Statistical analysis

All statistical tests were performed with SAS 9.4 (SAS Institute, Inc., Cary, NC). Percentage data were arcsine, square-root transformed before statistical analyses. Differences were considered significant at $p < 0.05$ for print failures. A three-factor analysis of variance (ANOVA, Proc Glimmix) was used to compare the effects of filament type

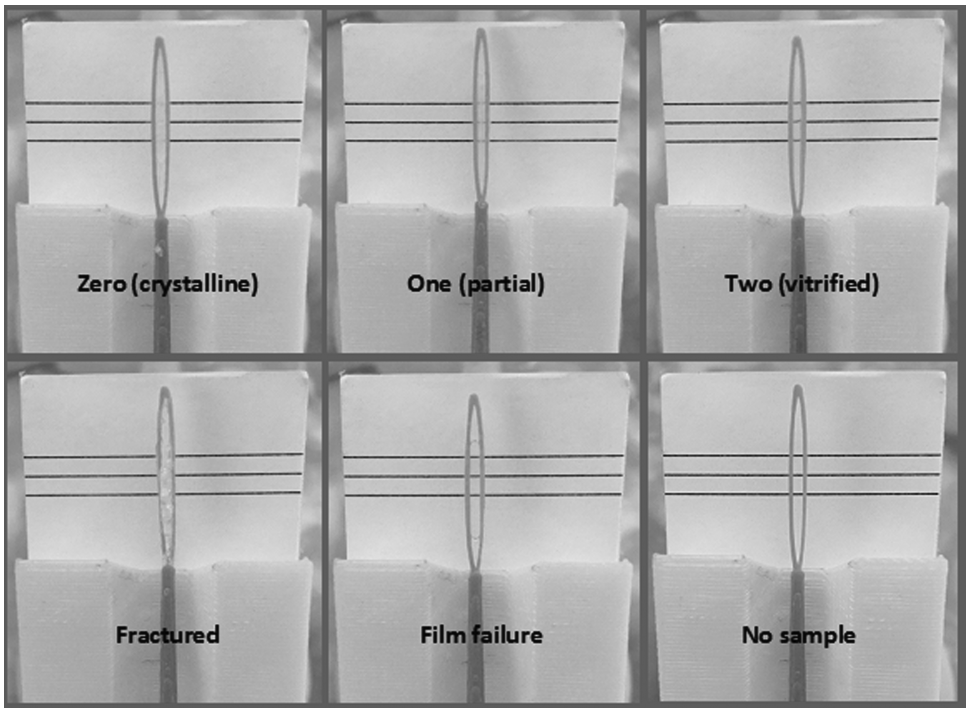

FIG. 3. Representative images of frozen films in prototype loops (Long, PLA) to illustrate the assessment classifications.[8] Frozen films were assigned a classification number: zero (opaque, or abundant crystalline ice formation); one (translucent, or partial vitrification); or two (transparent, or substantial vitrification, glass). ''Film fractures'' were recorded when visible cracks disabled the ability to properly assign a numerical classification. ''Film failures'' were recorded when films were disrupted during the freezing process, and sometimes residual sample was observed at the ends of these loops. PLA, polylactic acid.

(ABS and PLA), loop length (short, intermediate, and long), and nominal layer height (0.2, 0.4, 0.6, 0.8, 1, and 1.2 mm).

Differences in the loading volume between solution (water and vitrification), filament type (ABS and PLA), loop length (short, intermediate, and long), layer height (0.2, 0.6, and 1.2 mm), and loading method (pipetting and submersion) were analyzed using a five-factor ANOVA.

Logistic regression (Proc Logistic) was used to analyze the relationship between frozen film transparency (response variable) and loop configuration (independent variable). Submerged and pipetted loop classifications were combined, but layer heights of 0.4, 0.8, and 1 mm were excluded from the analyses to match the pipetted loop classification data. Film classification numbers 0 (opaque) and 1 (translucent) were grouped together and labeled as ''not transparent''; thus, film transparency followed a binary distribution (0 = not transparent, 1 = transparent). Loop configuration included filament type (ABS and PLA), loop length (short = 0, intermediate = 1, and long = 2), layer height (1 = 0.2, 3 = 0.6, and 6 = 1.2 mm), and volume (min, max, and submerged). The goodness-of-fit of the logistic regression model was assessed by the Hosmer–Lemeshow goodness-of-fit test.

For the submerged loading of loops, differences in film failure rate and sample thaw time were analyzed using a three-factor ANOVA (filament type, loop length, and layer height). Differences in fill time, film failure rate, and sample thaw time of pipetted loops were analyzed using a four-way ANOVA (filament type, loop length, layer height, and volume).

Results

Print failure rate

Failure to print two successful replicates of each configuration was significantly different between ABS and PLA ($p < 0.001$) (Table 1). Failure rate for ABS was 5% ± 16% (mean ± SD) and for PLA was 31% ± 25%. Slight variations in layer height and width (~0.05 mm) were observed in replicates of printed objects from each other or from the programmed sizes.

Table 1. Failure Rates to Print Two Replicates of Each Configuration with Two Filament Types (ABS and PLA)

	Short		*Intermediate*		*Long*		
Number of layers	*ABS, %*	*PLA, %*	*ABS, %*	*PLA, %*	*ABS, %*	*PLA, %*	*Mean ± SD, %*
1	0	60	0	50	0	33	24 ± 28
2	33	50	60	0	0	0	24 ± 28
3	0	71	0	60	0	33	27 ± 32
4	0	33	0	0	0	50	14 ± 22
5	0	60	0	0	0	0	10 ± 25
6	0	33	0	0	0	33	11 ± 17
Mean ± SD, %	6 ± 14	52 ± 16	10 ± 25	18 ± 29	0 ± 0	25 ± 20	

Configurations consisted of six nominal heights (0.2 mm/layer) and three lengths (short—15 mm, intermediate—19 mm, and long—23.5 mm).

ABS, acrylonitrile butadiene styrene; PLA, polylactic acid.

Loading volumes by submersion and pipetting

Two replicates for each loop configuration were recorded for a total of 198 samples (Fig. 4). The loading volumes were significantly different between solution type, loop length, layer height, and loading method ($p < 0.001$), but filament type was not significant ($p = 0.079$). The volume averaged across all configurations and both loading methods for vitrification solution was $7.2 \pm 4.4\,\mu$L and for water was $6.1 \pm 4.6\,\mu$L. For loop length averaged across all layer heights (1–6) and both loading methods, the mean volume was $5.5 \pm 3.8\,\mu$L for short, $6.4 \pm 4.3\,\mu$L for intermediate, and $7.9 \pm 5.1\,\mu$L for long. For layer height averaged with all loop lengths and both loading methods, the mean volume was $2.4 \pm 1.0\,\mu$L for 0.2 mm, $6.1 \pm 2.6\,\mu$L for 0.6 mm, and $11.3 \pm 3.4\,\mu$L for 1.2 mm. For loading method averaged across all configurations, the pipetted minimum volume was $4.6 \pm 2.5\,\mu$L, the pipetted maximum volume was $8.2 \pm 4.6\,\mu$L, and the submerged volume was $6.4 \pm 5.0\,\mu$L.

Frozen film classification

Logistic regression of frozen film transparency for loop configuration indicated that loop length ($p = 0.044$) and layer height ($p < 0.001$) were each significant, but filament type ($p = 0.465$) and volume ($p = 0.915$) were not significant. This suggested that as loop length increased, the probability of vitrifying increased, and as layer height increased, the probability of vitrification decreased (Fig. 5). The Hosmer–Lemeshow goodness-of-fit test ($\chi^2 = 3.75$, d.f. = 7, $p = 0.808$) showed good prediction of the logistic model.

Submerged loop characteristics

The processing times to load and freeze 144 samples (Table 2) were recorded after every third sample (average recorded time was 71 ± 27 s), due to the rapid processing of submerged loops. Film failure after freezing was significantly different between ABS and PLA ($p = 0.004$) and among layers ($p = 0.048$), but there was no significant difference for length ($p = 0.117$). Mean film failure rate for ABS was 0% and for PLA was $10\% \pm 16\%$. Thawing time was affected significantly by filament type ($p < 0.001$), layer height ($p < 0.001$), and the interaction of loop length, layer height, and filament type ($p = 0.016$), but was not affected by loop length ($p = 0.839$) or the interaction of loop length and layer height ($p = 0.969$), loop length and filament type ($p = 0.254$), and filament type and layer height ($p = 0.124$).

Pipetted loop characteristics

The time it took to pipette the maximum and minimum volumes for individual vitrification devices was recorded for a total of 72 samples (Table 3). Pipette filling times were affected significantly by filament type ($p = 0.004$), but not by volume ($p = 0.391$), loop length ($p = 0.081$), or layer height

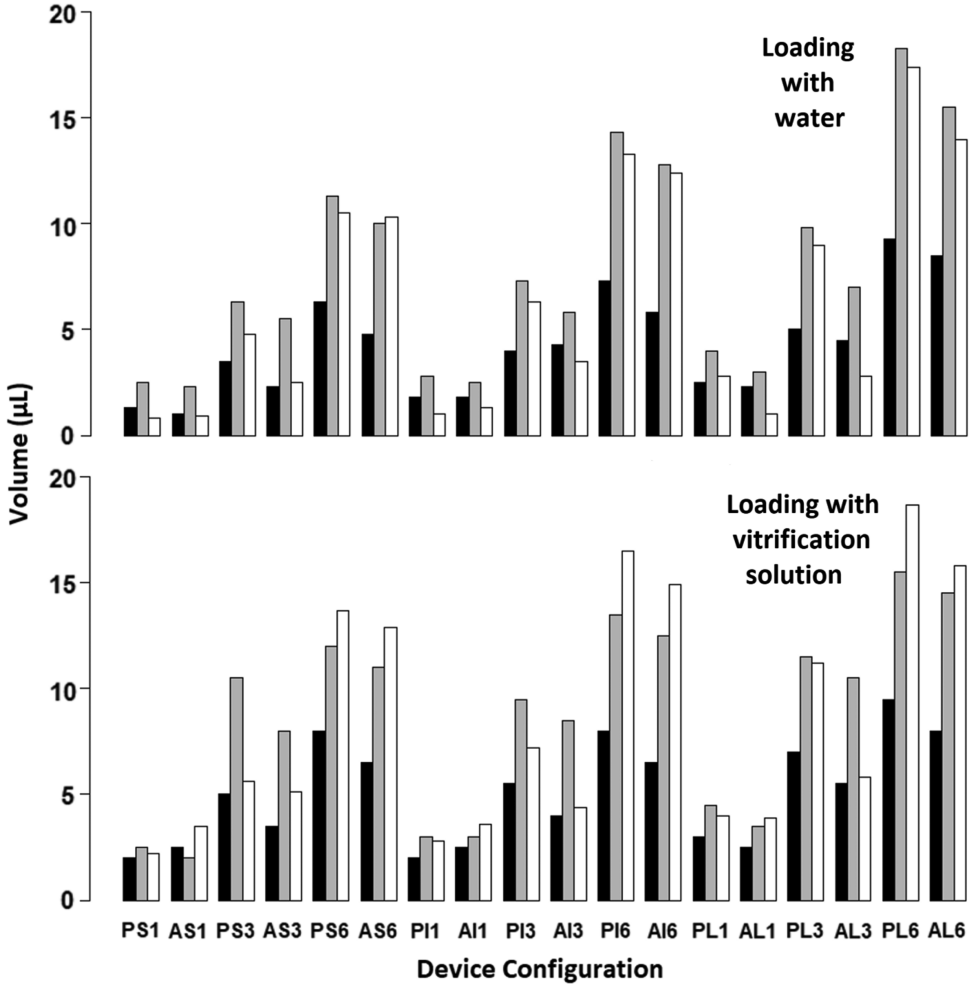

FIG. 4. The mean pipetted minimum (*black bars*), pipetted maximum (*gray bars*), and submerged (*white bars*) volumes of water (*upper graph*) and vitrification solution (*lower graph*) for different device configurations. Filament type, loop length, and layer height are identified by two letters and one number: the first letter indicates filament type, P (PLA) and A (ABS); the second letter indicates loop length, S (short), I (intermediate), and L (long); and the number indicates layer height, 1 (single layer), 3 (three layers), or 6 (six layers).

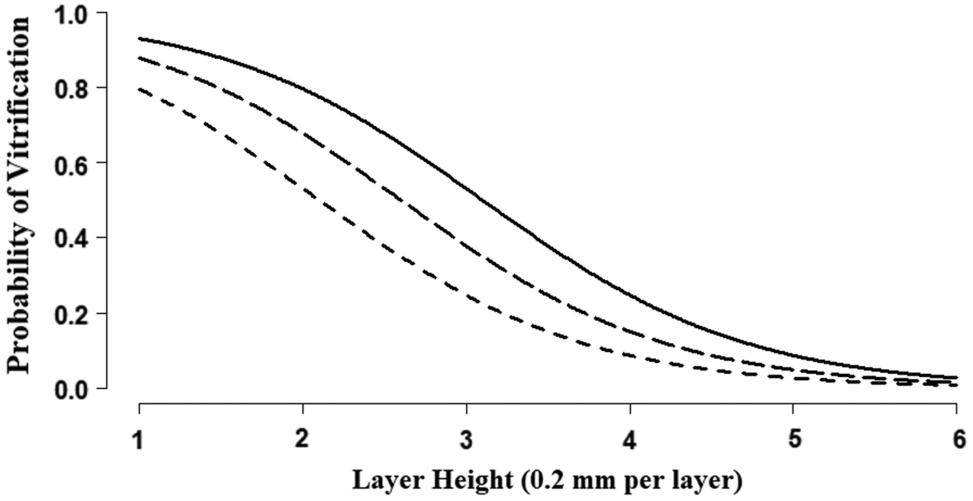

FIG. 5. Predicted probability of achieving vitrified (clear) samples for submerged and pipetted filling of long (*solid line*), intermediate (*long dashed line*), and short (*short dashed line*) prototype loops plotted against layer height. A probability of 0 represented opaque, 0.5 was translucent, and 1 was transparent (vitrified).

($p = 0.441$). The mean filling time for ABS was 69.3 ± 31.1 s and for PLA was 95.4 ± 44.2 s. There were no differences in film failure rate among all variables. Thawing time was significantly different among volumes ($p = 0.002$) and layer height ($p < 0.001$), but not filament type ($p = 0.622$) or loop length ($p = 0.686$). Mean thawing time for the minimum volume was 3.9 ± 1.1 s and the maximum volume was 4.7 ± 1.8 s. For layer height, the mean thawing time was 2.8 ± 0.5 s for 0.2 mm, 4.2 ± 1 s for 0.6 mm, and 5.7 ± 1.4 s for 1.2 mm.

Discussion

Vitrification encompasses a complex interplay of numerous factors, including physical, biological, and practical. Physical factors would include glass transition temperature (TG), surface area-to-volume ratios, and heat transfer properties of materials. Biological factors would include toxicity of cryoprotectants to cells, solution effects, and dehydration. Practical factors would include cell concentrations relative to sperm production, sperm-to-egg-ratios, and the number of eggs per female. These represent a subset of the simultaneously interacting variables that would need to be balanced against factors such as unit cost per device, and sample labeling, storage, shipping, and ease of thawing. As such, maximum flexibility to prototype and test new configurations coupled with inexpensive fabrication would be desirable features.

Currently, there are more than 25 devices and approaches available for vitrification of mammalian embryos[9] and would theoretically be available for use with aquatic species

Table 2. Submerged Loops of Two Filament Types (ABS and PLA) Received Classifications of Vitrification Quality

		Film failure		*Thaw time (s) ± SD*		*Classification*	
Length	*Layer*	*ABS, %*	*PLA, %*	*ABS*	*PLA*	*ABS*	*PLA*
Short	1	0	20	3.4 ± 0.5	3.2 ± 0.3	2, 2, 2, 2	1, 1, 2, 1
	2	0	0	3.7 ± 0.5	3.4 ± 0.4	1, 1, 2, 1	2, 2, 2, 2
	3	0	20	3.9 ± 0.7	3.9 ± 0.5	1, 2, 1, 1	1, 2, 1, 0
	4	0	0	4.9 ± 0.8	3.5 ± 0.6	0, 1, 1, 1	1, 1, 1, 1
	5	0	0	5.7 ± 1.3	4.7 ± 1.1	0, 1, 0, 0	0, 0, 0, 0
	6	0	0	5.2 ± 1.0	5.3 ± 1.5	1, 0, 1, 0	1, 1, 0, 0
Intermediate	1	0	20	3.3 ± 0.7	3.0 ± 0.5	2, 2, 2, 2	2, 2, 2, 2
	2	0	0	3.7 ± 0.6	3.4 ± 0.1	1, 1, 2, 1	1, 1, 2, 2
	3	0	0	4.1 ± 0.4	3.4 ± 0.1	0, 1, 2, 1	1, 1, 2, 2
	4	0	0	4.7 ± 0.4	4.2 ± 1.0	1, 0, 1, 1	1, 2, 2, 0
	5	0	0	5.7 ± 1.0	4.3 ± 0.6	0, 1, 1, 0	0, 1, 1, 1
	6	0	0	6.4 ± 2.0	4.7 ± 0.3	0, 0, 0, 0	0, 0, 0, 0
Long	1	0	43	2.8 ± 0.3	3.5 ± 0.5	2, 2, 2, 2	0, 2, 2, 2
	2	0	0	3.3 ± 0.5	3.3 ± 0.2	2, 2, 2, 1	2, 2, 2, 2
	3	0	43	3.5 ± 0.3	3.8 ± 0.6	2, 2, 2, 1	2, 1, 1, 2
	4	0	0	4.3 ± 0.9	3.9 ± 0.6	1, 1, 1, 0	1, 1, 2, 2
	5	0	33	4.8 ± 0.6	5.6 ± 1.0	0, 1, 0, 0	0, 0, 0, 0
	6	0	0	6.7 ± 1.2	4.3 ± 0.6	0, 0, 0, 0	0, 0, 0, 0

Rates of film failures and average film thaw times for each configuration were calculated. Assigned classifications were determined by transparency of frozen films (0—opaque, 1—translucent, and 2—transparent). Configurations consisted of six layer heights (0.2 mm/layer) and three lengths (short—15 mm, intermediate—19 mm, long—23.5 mm).

Table 3. Pipetted Minimum (Min) and Maximum (Max) Volumes of Selected Loop Prototypes in Two Filament Types (ABS and PLA) Received Classifications of Vitrification Quality

			Fill time (s)		*Film failure (%)*		*Thaw time (s) ± SD*		*Classification*	
Length	*Volume*	*Layers*	*ABS*	*PLA*	*ABS*	*PLA*	*ABS*	*PLA*	*ABS*	*PLA*
Short	Min	1	76 ± 18	101 ± 20	0	33	2.7 ± 0.2	3.3 ± 1.5	1, 2	1, 2
		3	40 ± 14	90 ± 32	0	0	4.8 ± 0.1	3.8 ± 1.7	0, 1	2, 2
		6	90 ± 56	59 ± 13	0	0	5.0 ± 0.5	4.4 ± 1.4	0, 0	0, 1
	Max	1	61 ± 13	49 ± 17	0	33	3.2 ± 0.0	2.8 ± 0.2	2, 2	2, 2
		3	51 ± 13	96 ± 26	0	0	5.0 ± 0.2	4.4 ± 0.8	1, 1	1, 0
		6	54 ± 54	64 ± 23	0	0	6.2 ± 1.9	7.2 ± 1.5	0, 0	0, 1
Intermediate	Min	1	63 ± 24	124 ± 27	0	0	2.6 ± 0.1	2.8 ± 0.0	2, 2	2, 2
		3	54 ± 4	84 ± 14	0	0	4.2 ± 0.5	3.4 ± 0.0	1, 1	2, 2
		6	51 ± 2	176 ± 13	33	0	4.8 ± 0.6	4.6 ± 1.0	1, 0	0, 0
	Max	1	83 ± 17	144 ± 44	0	0	2.7 ± 0.0	3.0 ± 0.9	2, 2	2, 2
		3	43 ± 11	99 ± 74	0	0	4.4 ± 1.1	3.9 ± 0.3	1, 2	2, 2
		6	81 ± 18	121 ± 82	0	0	7.6 ± 1.1	6.0 ± 0.4	1, 0	0, 0
Long	Min	1	70 ± 5	68 ± 23	0	0	2.6 ± 0.1	3.0 ± 1.4	2, 2	2, 2
		3	66 ± 37	138 ± 10	0	0	3.9 ± 0.5	3.1 ± 0.1	0, 1	1, 2
		6	124 ± 69	81 ± 36	0	50	4.1 ± 0.2	5.2 ± 0.7	1, 1	1, 2
	Max	1	105 ± 42	99 ± 44	0	0	2.6 ± 0.3	2.7 ± 0.7	2, 2	2, 2
		3	80 ± 37	52 ± 11	0	0	5.1 ± 1.1	6.1 ± 0.0	1, 0	0, 1
		6	59 ± 4	75 ± 77	0	0	7.0 ± 0.1	6.8 ± 1.0	0, 0	0, 0

Rates of film failures and average film thaw times for each configuration were calculated. Assigned classifications were determined by transparency of frozen films (0—opaque, 1—translucent, and 2—transparent). Configurations consisted of three heights of layers (0.2 mm/layer) and three lengths (short—15 mm, intermediate—19 mm, and long—23.5 mm).

vitrification. They range in unit cost from about $0.06 to $20 and cover a range of volumes and configurations (some manufactured, others fabricated in the laboratory).

Currently, research on an application such as zebrafish sperm vitrification would begin with a survey of the available devices. This approach was used in a comprehensive baseline project to develop generalized methods for aquatic species vitrification,[10] which ultimately focused on research of 10-μL plastic bacteriological inoculation loops, and in a recent study in freshwater and marine fishes.[11] This latter study concluded that Cryotops (a specific proprietary device used for human embryos) were most successful for fish sperm (including comparison to 10-μL inoculation loops). Cryotop devices (www.kitazato-dibimed.com) cost $\sim$$20 each and were used for freezing 2 μL of sample, features that would have limited practicality for widespread application with aquatic species.

The use of 3D printing can produce devices that provide comparable physical conditions to all the approaches above at a cheaper per-unit cost, enables full customization of devices to suit the exact needs of a particular application, and can proceed directly from prototyping to fabrication on the same machine. Successful designs or devices can be exchanged electronically by sharing of files that can be used to print identical devices at multiple locations. This is clearly a more useful and efficient approach than the currently available methods, which rely on hit-or-miss empirical survey of devices designed for other uses in other taxa.

If we look at the previous example in practical terms, such as if we chose to freeze a total of 1000 μL of sample (e.g., 100 μL each for 10 males), we would need 500 Cryotops (2 μL each) at a total cost of $10,000, or we could use 70 3D printed devices (15 μL each) at a total material cost of >$1 (or for the same total cost, produce $\sim$800,000 3D printed vitrification devices). In such a comparison, cost savings could be used to purchase a 3D printer (at $250–$2,500) that could be used to fabricate established devices, and to prototype and customize new devices for vitrification or other cryobiological applications. However, if instead of using Cryotops, we chose to use the cheaper 10-μL microbiological inoculation loops ($\sim$$0.10 each), we would be presented with a hit-or-miss situation where they would either be effective or not for vitrification. In addition, 3D printing enables not only customization of the sample-containing structure (e.g., loop volume, material, and configuration) greatly enhancing the potential for vitrification success but would also enable customization of the rest of the device, including handle geometry and intrinsic identification markings or other labeling.

There are at least 10 zebrafish vitrification studies published over the past 20 years (Table 4). The studies were done for a variety of purposes and addressed a range of tissues: ovarian follicles, embryos, blastomeres, primordial germ cells, and fin explants. As is typical for cryopreservation reports,[12] it is problematic to directly compare these studies because terms are not standardized (e.g., ''survival'' and ''viability'') and details are not provided on practical features such as unit cost per device. Surprisingly, we did not find published work on zebrafish sperm vitrification, although the small sperm volumes of these fishes coupled with the small egg numbers (100 or less) per female make them ideally suited for vitrification.

The devices used to conduct these studies were either not specifically designed for aquatic species cryopreservation or were handcrafted in the laboratory, which complicates advancement of zebrafish vitrification through the lack of published information with relevant devices. To address these drawbacks, the use of 3D printing technology presents a viable platform to provide vitrification (and other cryopreservation related) devices specifically designed for biomedical and other aquatic species.

TABLE 4. LITERATURE REVIEW OF PREVIOUS STUDIES USING VITRIFICATION WITH ZEBRAFISH

Study	*Purpose of study*	*Device used*	*Purpose or source of device*	*Sample volume*	*Material*	*Results*[a]	*Unit device cost*[b]
Zhang and Rawson 1996[17]	Embryos (12 and 27 h)	0.25-mL French straw	Semen freezing	~40 μL	Plastic	No viability	$0.06 (2,000 pk.)
Robles at al.[18]	Embryos (3 and 12 h)	0.5-mL straw	Semen freezing	?	Plastic	No hatching	$0.06 (2,000 pk.)
Cardona-Costa *et al.*[19]	Caudal fin explants	0.25-mL straw	Semen freezing	?	Plastic	Culture possible	$0.06
Cardona-Costa *et al.*[20,21]	Blastomeres	2.5-cm filament loop	Laboratory crafted	~0.25 μL	Nylon	>70% survival	?
Guan *et al.*[22]	Oocytes (stage III)	0.25-mL straw	Semen freezing	0.25 mL	Plastic	Severe damage	$0.06
		CryoLogic hook	Vitrification	5–10 μL	Proprietary	Severe damage	$5.50 (100 pk.)
		Fibreplug™					
Higaki *et al.*[23,24]	PGC recovery from vitrified embryos	100-μm mesh	Laboratory crafted	Minimal	Nylon	~50% recovery	?
Godoy *et al.*[25]	Stage III ovarian follicles	0.25-mL French straw	Semen freezing	0.25 mL	Plastic	No survival	$0.06
		CryoLogic hook	Vitrification	0.5 μL	Proprietary	No survival	$5.50
		fibreplug					
Marques *et al.*[26]	Ovarian follicles (five stages)	Two-piece, custom-built chambers	Vitrification	Minimal	Stainless steel	<38% survival	?

The studies were performed for a variety of purposes with various devices, most not designed for use with zebrafish. These devices were made with a variety of materials and yielded a range of results that were often difficult to compare on the basis of cost per device.

[a]Survival assessments based on observations made at >24 h after thawing.

[b]Unit cost per device based on smallest pack sizes (pk.) available from commercial suppliers.

PGC, primordial germ cells.

Design of prototype vitrification loops with varied dimensions

The design of versatile devices presents a system of tradeoffs in functionality and physical attributes, and the production of functional, convenient, and sturdy devices requires balancing of vitrification performance with user capabilities. The prototype loops designed in this study were within the diameter of standard 0.5-mL French straws, thus constraining the loops into an elliptical shape. This major constraint provided the advantages of traditional storage methods, and triangular handles aided spacing and compact storage within standard plastic goblets. Vitrification typically requires small (μL) volumes and our prototype loops were designed to address this range (i.e., 1–19 μL), balancing sample volume against the insulation created by thermoplastic mass.

Printing of prototype loops for testing

Previous work in 3D printing of freezing devices has shown PLA to be especially suited for cryogenic applications,[6] and this report identifies ABS as also being suitable. These thermoplastics did not change shape or lose structural integrity[7] when plunged into liquid nitrogen or after thawing. Other thermoplastic filament materials are available for 3D printing, but are not as commonly used as PLA and ABS, and the cryogenic responses of those materials in printed form should be evaluated. In this study, the PLA filament had a higher failure rate when printing vitrification devices (Table 1) under the conditions we used. Devices printed with longer and taller loops (five or more layers, intermediate to long lengths) proved easiest to print. Failed prints occurred most frequently when the printer head attempted to connect the initial layers of the loop to the neck.

Humidity levels can play a factor in the success of 3D printing, and increased humidity can reduce the ability of filament to extrude evenly, so the layers can become misplaced on the build plate.[13] Despite the use of a room dehumidifier, humidity levels may have still been a factor. The MakerBot Replicator 2X printer has a heated building plate, which supports the extrusion process. This may have provided an advantage for the devices printed with ABS over those printed with PLA.

Another inherent feature of the printing process is the slight variation (~0.05 mm) in layer height and width that is sometimes encountered when printing repeated objects, or as a departure from programmed sizes. These variations are relatively less important as the size of a printed object increases, and can be addressed by control measures, including use of high quality filament, proper maintenance and training, and higher resolution (i.e., more expensive) 3D printers and settings. This variation did not affect the overall results of this study of prototype loops, but should be considered a quality control checkpoint within a quality assurance program for cryopreservation activities, and would be of greater concern when using very thin or short loops or devices.

Evaluation of loading methods

The method used to load devices can affect the throughput and reliability of vitrification. Submersion was the more efficient method of loading, but it yielded a less consistent range of volumes compared to pipetting. Devices loaded by pipetting would thus have more consistent film volumes with

less film failures. The wetting properties of plastic filament types are used to describe the interaction between plastic and liquid. Engineers use contact angle to quantify the relationship of a droplet to a surface; contact angles can be used to describe a material as being hydrophilic (contact angles <90°) or hydrophobic (contact angles >90°).[14] Pure ABS and PLA materials each have good wetting ability (generally hydrophilic), while ABS is slightly more hydrophobic.[15,16] This may account for the data presented showing ABS with a lower frequency of film failures, but thermoplastic filaments contain a variety of other materials such as pigments and plasticizer agents that can affect wetting characteristics.

The availability of alternative methods of loading provides flexibility for experimentation, as each loading method offered different weaknesses and advantages. Pipetting allowed higher levels of reproducibility and accuracy when measuring the volume capacities of loops (such as would be done for quality control and reporting of data). Pipetting of deionized water into loops offers a precise measurement of liquid volume that could be used universally, lending itself to standardization of loop characterization and for international research. Submersion was easily the more efficient method of loading, and could minimize the time gametes are exposed to toxic vitrification solutions. Films formed through submersion typically yielded volumes somewhere between the pipetted maximum and minimum volumes. Submersion also enhanced throughput, while requiring less training and effort, making it a practical method of loading with time constraints, and would probably be most useful for application of vitrification, especially under field conditions.

Classification of vitrification quality

Most of the prototype vitrification loops tested in these studies provided vitrification at least once with one loading method; this clearly demonstrates the feasibility of using 3D printed vitrification loops in these size ranges and configurations. Currently available vitrification devices offer little diversity of volume capacity in loops, but 3D printing allows a user to print custom ranges of loop sizes and shapes. 3D printing offers an approach to customize ideal configurations of vitrification devices, with rapid design, prototyping, and testing, dependent upon the variables encountered when freezing. These configurations could be standardized within user groups to provide quality control and a consistent basis for comparison of published results.

Major factors that affected vitrification performance were loop volume and configuration. Increased volumes presumably required more time to freeze, which allowed ice crystallization to occur. Taller loops insulated the solution and diminished the ability to transfer heat effectively. Typically, loop configurations that held larger volumes tended to yield lower vitrification quality, compared to films holding smaller volumes. Configurations that paired the attributes of thin (one to three layers) and long loops tended to most consistently yield vitrification. The filament type did not significantly affect the frozen film quality or thaw times.

These studies demonstrate the potential for 3D printing to provide a ready means to both innovate and standardize methods of cryopreservation for aquatic species. Most vitrification devices currently available are designed for specific tasks unrelated to aquatic species, or have features that reduce vitrification quality. Combining 3D printing with cryopreservation can resolve many of the drawbacks that characterize devices currently available.[7] Diverse user groups would be able to optimize experimentation to their specifications. Files containing specific devices can be shared electronically, thus supporting development of connected communities formed internationally through social media.[6] Future studies would involve design and selection of optimized devices for biological testing of vitrification using samples such as sperm, and design of more sophisticated self-contained, and readily labeled, 3D printed vitrification devices.

Continued use of the empirical survey approach of available vitrification devices greatly hinders research by limiting experimental options for study of main effects (e.g., testing across a range of values for single or multiple variables), and only allows single comparisons of ''one-off'' devices or methods, constraining development of a mechanistic understanding of phenomena relevant to vitrification. For example, what is the effect of sample volume on vitrification success? This is a study not easily performed with a device only available with a set 10-μL volume. Such an approach would also not allow the study of the effects of loop shape on the stability of thin films during freezing, or the insulating effects of loop material on glass formation.

Each of these questions could be evaluated and optimized through 3D printing of a graduated series of devices for testing, and can be coupled or assisted by use of numerical modeling for design and mechanism elucidation. None of this core scientific activity is possible through surveying devices only available ''off the shelf,'' and it significantly limits options for application due to a lack of customization ability. Fabrication by 3D printing provides a technology platform that will allow the development of thousands of options for cryobiological work to proceed along a trajectory of innovation to customization to standardization. Initially, in this specific case, 3D printed devices can be developed to vitrify any tissue or cell type. These prototypes can be rapidly tested, optimized, and customized. With acceptance throughout user communities, particular devices can be standardized for functional considerations (e.g., volumes and geometry) and for features such as labeling, storage, and price. Indeed, it may be useful when evaluating vitrification devices in the future to include comparisons made on the basis of unit cost (e.g., per μL) of vitrified sample.

Acknowledgments

This work was supported, in part, by funding from the National Institutes of Health, Office of Research Infrastructure Programs (R24-RR023998 and R24-OD011120), with additional support provided by the National Institute of Food and Agriculture, United States Department of Agriculture (Hatch project LAB94231) and the LSU/ACRES Collaborative Project. This report was approved for publication by the Director of the Louisiana Agricultural Experiment Station as number 2016-241-30594. We thank W.T. Monroe, J. Jenkins-Tiersch, M. Sigler, C.J. Tiersch, and T. Gutierrez-Wing for technical assistance.

Disclosure Statement

No competing financial interests exist.

References

1. Yavin S, Arav A. Measurement of essential physical properties of vitrification solutions. Theriogenology 2007; 67:81–89.
2. Cuevas-Uribe R, Yang H, Daly J, Savage MG, Walter RB, Tiersch TR. Production of F1 offspring with vitrified sperm from a live-bearing fish, the green swordtail *Xiphophorus hellerii*. Zebrafish 2011;8:167–179.
3. Hagedorn M, Lance S, Fonseca D, Kleinhans F, Artimov D, Fleischer R, *et al.* Altering fish embryos with aquaporin-3: an essential step toward successful cryopreservation. Biol Reprod 2002;67:961–966.
4. Cuevas-Uribe R, Leibo S, Daly J, Tiersch TR. Production of channel catfish with sperm cryopreserved by rapid non-equilibrium cooling. Cryobiology 2011;63:186–197.
5. Kuwayama M, Vajta G, Kato O, Leibo SP. Highly efficient vitrification method for cryopreservation of human oocytes. Reprod Biomed Online 2005;11:300–308.
6. Hu E, Childress W, Tiersch TR. 3-D printing provides a novel approach for standardization and reproducibility of freezing devices. Cryobiology 2017;76:34–40.
7. Tiersch TR, Monroe WT. Three-dimensional printing with polylactic acid (PLA) thermoplastic offers new opportunities for cryobiology. Cryobiology 2016;73:396–398.
8. Tiersch NJ, Tiersch TR. Standardized assessment of thin-film vitrification for aquatic species. N Am J Aquacult 2017;79:283–288.
9. Marco-Jiménez F, Jiménez-Trigos E, Almela-Miralles V, Vicente JS. Development of cheaper embryo vitrification device using the minimum volume method. PLoS One 2016;11:e0148661.
10. Kása E, Bernáth G, Kollár T, Żarski D, Lujić J, Marinović Z, *et al.* Development of sperm vitrification protocols for freshwater fish (Eurasian perch, *Perca fluviatilis*) and marine fish (European eel, *Anguilla anguilla*). Gen Comp Endocrinol 2017;245:102–107.
11. Kása E, Bernáth G, Kollár T, Lujić J, Marinović Z, Urbányi B, *et al.* Vitrification of fish sperm: investigation of the supposed positive effect of trehalose. Cryobiology 2016;73: 409.
12. Tiersch TR: Introduction to the second edition. In: Cryopreservation in Aquatic Species. Tiersch TR and Green C (eds), pp. 1–17, World Aquaculture Society, Baton Rouge, LA, 2011.
13. Ho K-LG, Pometto AL, Hinz PN. Effects of temperature and relative humidity on polylactic acid plastic degradation. J Polym Environ 1999;7:83–92.
14. Bascom WD. The wettability of polymer surfaces and the spreading of polymer liquids. In: Polymer Physics. pp. 89–124, Springer, Berlin, Germany, 1988.
15. Janorkar AV, Metters AT, Hirt DE. Modification of poly (lactic acid) films: enhanced wettability from surface-confined photografting and increased degradation rate due to an artifact of the photografting process. Macromolecules 2004;37:9151–9159.
16. Choi YS, Xu M, Chung IJ. Synthesis of exfoliated acrylonitrile–butadiene–styrene copolymer (ABS) clay nanocomposites: role of clay as a colloidal stabilizer. Polymer 2005;46:531–538.
17. Zhang T, Rawson DM. Feasibility studies on vitrification of intact zebrafish (*Brachydanio rerio*) embryos. Cryobiology 1996;33:1–13.
18. Robles V, Cabrita E, De Paz P, Cuñado S, Anel L, Herráez M. Effect of a vitrification protocol on the lactate dehydrogenase and glucose-6-phosphate dehydrogenase activities and the hatching rates of Zebrafish (*Danio rerio*) and Turbot (*Scophthalmus maximus*) embryos. Theriogenology 2004;61:1367–1379.
19. Cardona-Costa J, Roig J, Perez-Camps M, Garcia-Ximenez F. Vitrification of caudal fin explants from zebrafish adult specimens. Cryoletters 2006;27:329–332.
20. Cardona-Costa J, García-Ximénez F. Vitrification of zebrafish embryo blastomeres in microvolumes. Cryoletters 2007;28:303–309.
21. Cardona-Costa J, Francisco-Simão M, García-Ximénez F. Can vitrified zebrafish blastomeres be used to obtain germline chimaeras? CryoLetters 2009;30:422–428.
22. Guan M, Rawson D, Zhang T. Cryopreservation of zebrafish (*Danio rerio*) oocytes by vitrification. CryoLetters 2010;31:230–238.
23. Higaki S, Eto Y, Kawakami Y, Yamaha E, Kagawa N, Kuwayama M, *et al.* Production of fertile zebrafish (*Danio rerio*) possessing germ cells (gametes) originated from primordial germ cells recovered from vitrified embryos. Reproduction 2010;139:733–740.
24. Higaki S, Kawakami Y, Eto Y, Yamaha E, Nagano M, Katagiri S, *et al.* Cryopreservation of zebrafish (*Danio rerio*) primordial germ cells by vitrification of yolk-intact and yolk-depleted embryos using various cryoprotectant solutions. Cryobiology 2013;67:374–382.
25. Godoy LC, Streit DP, Zampolla T, Bos-Mikich A, Zhang T. A study on the vitrification of stage III zebrafish (*Danio rerio*) ovarian follicles. Cryobiology 2013;67:347–354.
26. Marques LS, Bos-Mikich A, Godoy LC, Silva LA, Maschio D, Zhang T, *et al.* Viability of zebrafish (*Danio rerio*) ovarian follicles after vitrification in a metal container. Cryobiology 2015;71:367–373.

Address correspondence to:
Terrence R. Tiersch, PhD
Aquatic Germplasm and Genetic Resources Center
School of Renewable Natural Resources
Louisiana State University Agricultural Center
2288 Gourrier Avenue
Baton Rouge, LA 70820

E-mail: ttiersch@agctr.lsu.edu